

Theoretical Study of the Influence of Electric Fields on Hydrogen-Bonded Acid–Base Complexes

Mar Ramos,^{†,‡} Ibon Alkorta,^{*,†} Jose Elguero,[†] Nicolai S. Golubev,[§] Gleb S. Denisov,[§] Hans Benedict,^{||} and Hans-Heinrich Limbach^{*,||}

Contribution from the Instituto de Química Médica, C.S.I.C., Juan de la Cierva 3, E-28006 Madrid, Spain, Institute of Physics, St. Petersburg State University, 198904 St. Petersburg, Russian Federation, and Institut für Organische Chemie, Takustrasse 3, Freie Universität Berlin, D-14195 Berlin, Germany

Received: August 7, 1997; In Final Form: October 2, 1997[⊗]

Matrix effects on the optimized geometries and the electronic properties of acid–base complexes XHB, with HX = HF, HCl, HBr, HCN and B = NH₃, have been modeled using ab initio methods (6-31G** and 6-311++G** basis sets) in two different ways. Model A corresponds to the Onsager SCRF model, and model B corresponds to a homogeneous electric field $F = 2qe_0/r_c^2 = 2.88 \times 10^5 q$ V/cm of varying strength generated by two distant charges $+qe_0$ and $-qe_0$ of opposite sign placed at distances of $r_c = 100$ Å. In both models, the minima and reaction coordinate of proton transfer has been calculated. As the electric interactions are increased, both models predict an increase of the dipole moments associated with a proton shift from X to B, i.e., a conversion of the molecular to the zwitterionic complexes. Both models predicts double minima for some electric fields; in model B electric fields are found where the neutral complex is not stable, evolving to the ion pair complex. These fields can be used to characterize the acidity of the donor toward the base without the necessity of assuming a proton-transfer equilibrium. In both models a similar field-induced correlation between the two hydrogen bond distances $r_1 \equiv X \cdots H$ and $r_2 \equiv H \cdots B$ is observed for all configurations. This correlation indicates in the molecular complexes a hydrogen bond compression when the proton is shifted toward the base and in the zwitterionic complexes a widening. The minimum of the $X \cdots B$ distance $r_1 + r_2$ occurs when the proton-transfer coordinate $r_1 - r_2 = r_{01} - r_{02}$, where r_{01} and r_{02} represent the distances $X \cdots H$ and $H \cdots B^+$ in the free donors.

Introduction

Hydrogen bonds are one of the most important forces for the structural organization of molecules in condensed phase. They define the 3D arrangement of macromolecules and their biological activity.¹ In hydrogen-bonded complexes XHB between an acid HX and a base B, proton transfers can take place that are the key steps of a large number of chemical and biochemical reactions.² Thus, numerous experimental and theoretical studies have been carried out to understand the properties of strong hydrogen bonds and the nature of the proton transfer in these bonds as a function of the environment.^{3,4}

Most of the ab initio calculations of hydrogen-bonded complexes XHB refer to isolated systems in the gas phase where the hydrogen bond geometries are often very different from those in condensed matter. The effect of external electric fields that can model the solvent effect on the hydrogen bonds have been studied by Scheiner et al.⁵ and Eckert and Zundel.⁶ In the first case, the potential energy surface of the proton transfer was studied using nonhomogeneous electric fields in systems where the heavy atom positions were fixed. The second study considered a homogeneous electric field over the BrH \cdots CH₃-NH₂ system. The energy and dipole moment surfaces were calculated as a function of the electric field. Kurnig and Scheiner examined the three X–H \cdots NH₃ cases (X = F, Cl, Br), taking into account solvent effects.⁷ They used the reaction field

susceptibility g [$g = (2/a^3)Y$, where a is the radius of the spherical cavity and Y is the Onsager function] to describe the solvent and a “proton transfer parameter” ρ [$\rho = \Delta r(XH) - \Delta r(NH)$, Δr 's being defined as differences between the complex and the isolated XH and NH₄⁺]. They show that an increase in g produces an increase in ρ (the proton is transferred when $\rho > 0$), the phenomenon being dependent on the nature of X (Br > Cl \gg F). The distance $X \cdots N$ decreases (contraction) when g increases (greater ionic character). Note, finally, that Scheiner's ρ is related to our $r_1 - r_2$ distance (Figure 1) [for the three complexes $(r_1 - r_2) = 0.996 + 2.712 \rho$, $r^2 = 1.000$]. Recently, Scheiner and Kar⁸ and Clementi et al.⁹ have modeled, using ab initio methods, solvent effects on XHB. Clementi contribution concerns very high level calculations of one of Scheiner's complexes, Cl–H \cdots NH₃. Since the experimental geometry was known ($d_{Cl-H} = 1.30$ Å, $d_{N-H} = 1.82$ Å, $d_{Cl-N} = 3.13$ Å), Clementi shows that MP2 or CCSD calculations with a very large basis set are necessary to reproduce exactly the experimental geometry (compare with Scheiner's MINI-1 results, $d_{Cl-H} = 1.44$ Å, $d_{N-H} = 1.58$ Å, and with our 6-311++G** results, $d_{Cl-H} = 1.29$ Å, $d_{N-H} = 2.01$ Å). Solvent effects were studied, using the SCRF method, for different values of e , maintaining the distance $d_{Cl-N} = 3.13$ Å.⁹ In the case of Scheiner and Kar,⁸ the complex was placed in the center of a spherical cavity surrounded by a continuous medium with a given dielectric constant ϵ . The reaction electric field generated by this model is proportional to the dipole moment of the solute in a medium of increasing dielectric constant, where the reactive electric field is generated using the Onsager SCRF formalism.¹⁰ As ϵ was increased, a proton-transfer equilibrium was predicted to arise between the molecular complexes XH \cdots B and zwitterionic complexes X[–] \cdots HB⁺, separated by an energy barrier that arises

[†]Instituto de Química Médica.

[‡] On leave from the Departamento de Química Orgánica I, Facultad de Química, Universidad Complutense de Madrid, Ciudad Universitaria s/n, E-28040 Madrid, Spain.

[§] Institute of Physics.

^{||} Institut für Organische Chemie.

* To whom correspondence should be addressed.

[⊗] Abstract published in *Advance ACS Abstracts*, November 15, 1997.

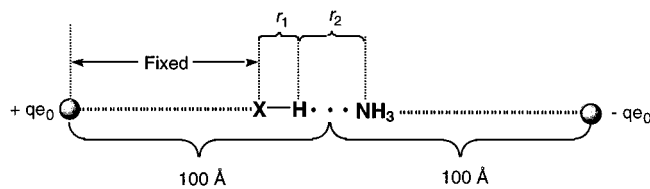


Figure 1. Schematic representation of model B consisting of a hydrogen-bonded acid–ammonia complex placed in a homogeneous electric field $F = 2qe_0/r_e^2 = 2.88 \times 10^5 q \text{ V cm}^{-1}$ created by two opposite charges $+qe_0$ and $-qe_0$ at distances of $r_e = 100 \text{ \AA}$ from the heavy atoms of the hydrogen bond. By comparison, an electric dipole μ creates a maximum electric field of $F = \mu/(4\pi r^3) = 2.40 \times 10^8 \mu/r_m^3$, where r is in \AA and μ in D. For example, a charge of $q = 200$ leading to an electric field of $5.76 \times 10^7 \text{ V cm}^{-1}$ corresponds to the electric field created by three dipoles of 5 D located at a distance of 4 \AA .

from the solvent reorientation.⁸ Here, we will refer to this model as “model A”. It is evident that this model does not apply to a hydrogen-bonded system on the time scale of slow solvent reorientation or to systems located in surfaces or in the solid state. For example, recently, hydrogen bond geometry changes have been observed experimentally in the case of homoconjugate hydrogen-bonded systems of the type AHA^- perturbed by potassium cations.¹¹ This cation effect was modeled in ab initio calculations by adding a Li^+ at different distances, creating an inhomogeneous electric field at AHA^- . In addition, recent liquid NMR studies of model complexes between pyridine as a base and organic acids also indicated the importance of an electric field increase created by solvent dipole ordering at low temperatures. These fields were assumed to induce dipole moments that lead in the case of molecular complexes to a hydrogen bond contraction and in the case of zwitterionic complexes to a widening, indicating that the hydrogen bonds in the former weaken and in the latter strengthen with increasing temperature.⁴

To further assist this interpretation, it is fruitful to explore a method that is able to describe theoretically the response of a single model hydrogen-bonded acid–base complex XHB to an applied well-defined electric field F to model an individual molecular site on a time scale of slow solvent reorientation. We chose, therefore, the simplest approach one can conceive, i.e., model B where the solutes XHB are placed in a homogeneous electric field $F = 2qe_0/r_e^2$ varying in strength generated by two electrical charges $+qe_0$ and $-qe_0$ of opposite sign at distances of $r_e = 100 \text{ \AA}$ away from the heavy atoms of the hydrogen bond as shown in Figure 1.

The scope of this paper is, therefore, to present the results of an ab initio study of hydrogen bonded acid–base complexes XHNH_3 , with $\text{HX} = \text{HF}, \text{HCl}, \text{HBr},$ and HCN , using both model approaches. After a short theoretical section the results will be presented and discussed.

Methods

The calculations were carried out at the Hartree–Fock (HF) level of theory using the standard 6-31G** and 6-311++G** basis sets.^{12,13}

The cavities of the studied systems used for the calculations in terms of model A were calculated by computing the 0.001 au electron density envelop of the gas-phase geometry and applying a scaling factor of 1.33 to obtain an estimate of the molecular volume.¹⁴ All the systems have been fully optimized including the SCRF effect using the Berny minimization algorithm as implemented in the Gaussian–94 program.¹⁵ The optimizations have been carried out using the tight option that increases the convergence criteria.

In model B the electric field $F = 2qe_0/r_e^2 = 2.88 \times 10^5 q \text{ V cm}^{-1}$ is generated by two point charges located $r_e = 100 \text{ \AA}$ away of the center of the hydrogen bond of the isolated complex as indicated in Figure 1. By comparison, an electric dipole μ at a distance r_m creates a maximum electric field of $F = m/4\pi r^3 = 2.40 \times 10^8 m/r_m^3$, where r_m is in \AA and μ in debye (D). For example, a charge of $q = 200$ leading to an electric field of $5.76 \times 10^7 \text{ V cm}^{-1}$ corresponds to the electric field created by three dipoles of 5 D located at a distance of 4 \AA . These electric fields are comparable to the ones generated by ions in solution. For example, a solution of lithium salt can generate an electric field as large as $16 \times 10^7 \text{ V cm}^{-1}$.¹⁶

The position of the charges, i.e., r_e is maintained constant for the rest of the calculations for each complex. To avoid convergence problems, the position of the atom X has been fixed in all the cases to its original position. The rest of the geometrical parameters of the complexes and the monomers were fully optimized, keeping a C_{3v} symmetry, with the HONDO-8 program,¹⁷ until the maximum gradient components were smaller than 0.0001. Thus, the geometrical parameters obtained correspond to the stationary points of lowest energy.

The proton potentials have been evaluated in both models by varying systematically the value of the X–H distance and optimizing the rest of the geometrical parameters. Thus, the second minimum has been located and the corresponding energetic differences between the two minima and the corresponding proton-transfer barrier have been obtained.

The topology of the electron density of the monomers and the hydrogen-bonded systems has been characterized using the atoms in molecules (AIM) methodology¹⁸ as implemented by Colosowski and co-workers¹⁹ in the Gaussian-94 program.

Finally, a field-induced correlation between the two hydrogen bond distances r_1 and r_2 in a hydrogen-bonded complex $\text{X–H}\cdots\text{B}$ (see Figure 1) is observed in this study as shown below, which can be described by

$$\exp\{(r_{01} - r_1)/b\} + \exp\{(r_{02} - r_2)/b\} = 1 \quad (1)$$

r_{01} and r_{02} represent the distances in the free donors HX and HB^+ . The parameter b is given by

$$b = [(r_1 + r_2)_{\min} - (r_{01} + r_{02})]/(2 \ln 2) \quad (2)$$

where $(r_1 + r_2)_{\min}$ represents a minimum distance $\text{X}\cdots\text{B}$. For the case of $\text{O–H}\cdots\text{O}$ and $\text{N–H}\cdots\text{N}$ hydrogen-bonded systems, $r_{01} = r_{02} = r_0$. For these cases Steiner et al.^{3h,i} have shown, using published neutron diffraction data, eq 1 to be valid in the case of weak hydrogen bonds. This correlation follows from the bond valence–bond length concept well established in crystallography.²⁰ Equation 1 can be rewritten as eq 3:

$$(r_1 + r_2) = 2r_{02} + (r_1 - r_2) + 2b \ln[1 + \exp\{(r_{01} - r_{02} - r_1 + r_2)/b\}] \quad (3)$$

Results

The effects of an increase of the dielectric constant ϵ in model A and those of the external homogeneous electric field in model B on the geometry, dipole moment, and electron density of the bond critical point of the monomers are assembled in Tables 1 and 2, respectively. Tables 3 and 4 show the geometric and electronic variations of the hydrogen-bonded complexes for both models obtained with the 6-31G** and 6-311++G** basis sets. In general, the external field provides a slightly larger variation with the most flexible basis set used, 6-311++G**, than with the 6-31G** basis set. For this reason, the results obtained will

TABLE 1: Monomers' Interatomic Distances (Å), Dipole Moments (μ , D), and Electronic Density on the Bond Critical Points (ρ_c , e) Calculated for Different External Electric Fields Using Model Aⁱ

F–H		6-311++G** ^b		
ϵ	F···H	μ	ρ_c	
1.0	0.897	2.03	0.396	
5.0	0.899	2.10	0.391	
10.0	0.900	2.11	0.390	
15.0	0.900	2.12	0.390	
100.0	0.900	2.13	0.389	
Cl–H		6-311++G** ^d		
ϵ	Cl···H	μ	ρ_c	
1.0	1.270	1.43	0.256	
5.0	1.271	1.53	0.255	
10.0	1.271	1.54	0.255	
15.0	1.271	1.55	0.255	
100.0	1.271	1.56	0.255	
NC–H		6-311++G** ^f		
ϵ	C···H	μ	ρ_c	
1.0	1.058	3.32	0.300	
5.0	1.060	3.65	0.297	
10.0	1.061	3.73	0.297	
15.0	1.062	3.75	0.297	
100.0	1.062	3.81	0.296	
Br–H		6-311++G** ^h		
ϵ	Br···H	μ	ρ_c	
1.0	1.408	1.14	0.205	
5.0	1.409	1.23	0.205	
10.0	1.409	1.24	0.205	
15.0	1.409	1.25	0.205	
100.0	1.409	1.26	0.205	

^a Solute radius used in this calculation: 2.34 Å. ^b Radius used: 2.38 Å. ^c Radius used: 2.86 Å. ^d Radius used: 2.86 Å. ^e Radius used: 2.78 Å. ^f Radius used: 3.07 Å. ^g Radius used: 3.03 Å. ^h Radius used: 3.12 Å. The corresponding values obtained for $\epsilon = 20.0, 25.0, 30.0, 40.0,$ and 50.0 D are between the ones for $\epsilon = 15.0$ and 100.0 D.

be discussed only for the larger basis set (the 6-31G** data are available on request from any of us).

Free Acids HX. The influence of electric fields on the bond distances of the monomers HX is minimal. In fact, the largest dielectric constant ϵ in model A (Table 1) or the strongest field F in model B (Table 2) only produces a lengthening of the HX bond similar to one observed in the formation of the hydrogen bonds $\text{XH}\cdots\text{B}$ in the absence of an electric interaction. This finding is consistent with other studies that have shown small bond distance differences between the gas phase and solvent model calculation for most of the molecules studied.^{21–24}

The analysis of the electron density on the bond critical points confirms the small influence of the external electric interactions on the characteristics of the chemical bonds of HX. In contrast, the dipole moments of the monomers monotonically increase with the electric field strength in model B. The changes are larger in the most polarizable compounds [HBr (216%) > HCl (122%) > HCN (88%) > HF (29%)]. The values in the parentheses indicate the relative increase of the dipole moments when increasing the electric field strength from zero to the largest value. In model A, the dipole moment variation is very small for all the systems, i.e., less than 15% (Table 1).

Acid–Ammonia Complexes $\text{XH}\cdots\text{NH}_3$. In contrast to the small changes produced by external electric fields on the monomers HX, larger variations of the geometries and the electronic distributions were found for the hydrogen-bonded acid–base complexes $\text{XH}\cdots\text{NH}_3$ with the 6-311++G** basis set.

TABLE 2: Monomers' Interatomic Distances (Å), Dipole Moments (μ , D), and Electronic Density on the Bond Critical Points (ρ_c , e) Calculated for Different External Electric Field $F = 2qe_0/r_c^2 = 2.88 \times 10^5 q \text{ V cm}^{-1}$ Using Model B

F–H		6-311++G**		
q	F···H	μ	ρ_c	
0.0	0.897	2.03	0.396	
100.0	0.899	2.09	0.394	
200.0	0.901	2.16	0.392	
300.0	0.903	2.22	0.389	
400.0	0.905	2.29	0.386	
500.0	0.908	2.35	0.383	
600.0	0.910	2.42	0.380	
700.0	0.913	2.49	0.377	
800.0	0.916	2.56	0.374	
900.0	0.920	2.63	0.370	
Cl–H		6-311++G**		
q	Cl···H	μ	ρ_c	
0.0	1.270	1.43	0.256	
100.0	1.272	1.62	0.255	
200.0	1.275	1.80	0.253	
300.0	1.278	1.99	0.252	
400.0	1.281	2.18	0.250	
500.0	1.285	2.37	0.247	
600.0	1.291	2.57	0.245	
700.0	1.296	2.76	0.242	
800.0	1.303	2.97	0.239	
900.0	1.310	3.18	0.236	
Br–H		6-311++G**		
q	Br···H	μ	ρ_c	
0.0	1.407	1.14	0.205	
100.0	1.409	1.40	0.204	
200.0	1.412	1.66	0.203	
300.0	1.415	1.92	0.202	
400.0	1.418	2.18	0.201	
500.0	1.423	2.45	0.199	
600.0	1.429	2.72	0.197	
700.0	1.436	3.00	0.195	
800.0	1.444	3.29	0.193	
900.0	1.453	3.60	0.190	
NC–H		6-311++G**		
q	C···H	μ	ρ_c	
0.0	1.058	3.32	0.300	
100.0	1.061	3.59	0.297	
200.0	1.063	3.90	0.296	
300.0	1.066	4.22	0.294	
400.0	1.069	4.54	0.292	
500.0	1.072	4.86	0.290	
600.0	1.076	5.19	0.288	
700.0	1.079	5.53	0.286	
800.0	1.084	5.88	0.283	
900.0	1.089	6.23	0.280	

The results using the latter set are illustrated in Figures 2–5. We first present the results obtained in terms of model B and then those for model A.

Results Obtained for Model B. A general analysis of the results indicates that by use of this model, two simultaneous minima could exist: the first one that can be described as $\text{XH}\cdots\text{NH}_3$ (stage I) and the second one in which the proton is transferred to the amonia ($\text{X}^-\cdots\text{H}\cdots\text{NH}_3^+$) (stage II). The external field applied destabilized the first minima and stabilized the second one. A value of the external field has been found for all the complexes studied here where a transfer of the proton is produced from stage I to stage II.

The molecular and ion-pair complexes are clearly separated by an energy barrier (4) and are characterized by the energy difference (5).

TABLE 3: Interatomic Distances (Å), Dipole Moments (μ , D), Electronic Density on the Bond Critical Points (ρ_c , e), Relative Energies $\Delta E = E(X^- \cdots NH_4^+) - E(XH \cdots NH_3)$ (kcal mol⁻¹) of Molecular Complexes $XH \cdots NH_3$ and the Corresponding Zwitterions $X^- \cdots NH_4^+$, and Proton-Transfer Barrier $\Delta E(X)^\ddagger = E(X^- \cdots H-NH_3^+)^\ddagger - E(X-H \cdots NH_3)$ Calculated Using Model A and the 6-311++G Basis Set^e**

F-H \cdots NH ₃ ^a														
ϵ	F \cdots H	F \cdots N	H \cdots N	μ	ρ_c (F \cdots H)	ρ_c (H \cdots N)	ϵ	F \cdots H	F \cdots N	H \cdots N	μ	ρ_c (F \cdots H)	ρ_c (H \cdots N)	
1.0	0.918	2.738	1.820	4.60	0.358	0.036	20.0	0.936	2.665	1.729	5.37	0.331	0.046	
2.0	0.924	2.710	1.786	4.90	0.349	0.039	25.0	0.936	2.663	1.727	5.39	0.331	0.046	
3.0	0.927	2.696	1.769	5.04	0.344	0.041	30.0	0.936	2.662	1.726	5.40	0.330	0.046	
5.0	0.930	2.682	1.753	5.18	0.339	0.043	40.0	0.936	2.661	1.725	5.41	0.330	0.046	
10.0	0.934	2.672	1.738	5.30	0.334	0.045	50.0	0.937	2.661	1.724	5.42	0.329	0.047	
15.0	0.935	2.667	1.732	5.35	0.332	0.046	100.0	0.937	2.659	1.722	5.44	0.329	0.047	
F $^- \cdots$ NH ₄ ⁺														
ϵ	F \cdots H	F \cdots N	H \cdots N	μ	ΔE	ϵ	F \cdots H	F \cdots N	H \cdots N	μ	ΔE			
1.0	---	---	---	---	---	5.0	1.956	2.975	1.019	11.55	28.79			
2.0	1.763	2.792	1.029	10.12	37.33	10.0	+++	---	---	---	---			
3.0	1.841	2.864	1.023	10.74	33.17	---	---	---	---	---	---			
Cl-H \cdots NH ₃ ^b														
ϵ	Cl \cdots H	Cl \cdots N	H \cdots N	μ	ρ_c (Cl \cdots H)	ρ_c (H \cdots N)	ϵ	Cl \cdots H	Cl \cdots N	H \cdots N	μ	ρ_c (Cl \cdots H)	ρ_c (H \cdots N)	
1.0	1.292	3.307	2.015	4.19	0.242	0.026	20.0	1.329	3.117	1.788	5.49	0.218	0.044	
2.0	1.300	3.251	1.951	4.58	0.237	0.030	25.0	1.331	3.109	1.778	5.54	0.217	0.045	
3.0	1.305	3.220	1.915	4.79	0.233	0.032	30.0	1.333	3.104	1.771	5.58	0.216	0.046	
5.0	1.312	3.185	1.873	5.02	0.229	0.036	40.0	1.335	3.095	1.760	5.64	0.214	0.047	
10.0	1.321	3.147	1.826	5.29	0.223	0.040	50.0	1.337	3.089	1.752	5.68	0.213	0.048	
15.0	1.326	3.129	1.803	5.41	0.220	0.042	100.0	1.342	3.073	1.731	5.79	0.210	0.050	
Cl $^- \cdots$ NH ₄ ⁺														
ϵ	Cl \cdots H	Cl \cdots N	H \cdots N	μ	ΔE	barrier	ϵ	Cl \cdots H	Cl \cdots N	H \cdots N	μ	ΔE	barrier	
1.0	---	---	---	---	---	---	3.0	2.027	3.077	1.050	13.17	-5.71	1.39	
2.0	1.896	2.968	1.072	11.88	-0.88	2.91	5.0	+++	---	---	---	---	---	
NC-H \cdots NH ₃ ^c														
ϵ	C \cdots H	C \cdots N	H \cdots N	μ	ρ_c (C \cdots H)	ρ_c (H \cdots N)	ϵ	C \cdots H	C \cdots N	H \cdots N	μ	ρ_c (C \cdots H)	ρ_c (H \cdots N)	
1.0	1.070	3.301	2.231	5.73	0.293	0.016	20.0	1.080	3.210	2.130	6.79	0.286	0.020	
2.0	1.073	3.266	2.193	6.14	0.290	0.018	25.0	1.081	3.209	2.128	6.81	0.285	0.020	
3.0	1.075	3.249	2.174	6.34	0.289	0.018	30.0	1.081	3.208	2.127	6.83	0.285	0.021	
5.0	1.078	3.234	2.156	6.53	0.288	0.019	40.0	1.081	3.206	2.125	6.85	0.285	0.021	
10.0	1.079	3.218	2.139	6.70	0.286	0.020	50.0	1.081	3.205	2.124	6.86	0.285	0.021	
15.0	1.080	3.213	2.133	6.76	0.286	0.020	100.0	1.082	3.204	2.122	6.88	0.285	0.021	
NC $^- \cdots$ NH ₄ ⁺														
ϵ	C \cdots H	C \cdots N	H \cdots N	μ	ΔE	ϵ	C \cdots H	C \cdots N	H \cdots N	μ	ΔE			
1.0	---	---	---	---	---	5.0	---	---	---	---	---			
2.0	---	---	---	---	---	10.0	+++	---	---	---	---			
3.0	---	---	---	---	---	---	---	---	---	---	---			
Br-H \cdots NH ₃ ^d														
ϵ	Br \cdots H	Br \cdots N	H \cdots N	μ	ρ_c (Br \cdots H)	ρ_c (H \cdots N)	ϵ	Br \cdots H	Br \cdots N	H \cdots N	μ	ρ_c (Br \cdots H)	ρ_c (H \cdots N)	
1.0	1.428	3.518	2.090	3.96	0.199	0.023	20.0	1.450	3.372	1.922	4.87	0.191	0.033	
2.0	1.434	3.469	2.035	4.26	0.197	0.025	25.0	1.450	3.367	1.917	4.90	0.190	0.033	
3.0	1.438	3.444	2.006	4.42	0.196	0.027	30.0	1.451	3.365	1.914	4.92	0.190	0.033	
5.0	1.442	3.417	1.975	4.59	0.194	0.029	40.0	1.452	3.362	1.910	4.94	0.190	0.034	
10.0	1.446	3.389	1.943	4.76	0.192	0.031	50.0	1.452	3.359	1.907	4.95	0.190	0.034	
15.0	1.448	3.378	1.930	4.84	0.191	0.032	100.0	1.453	3.355	1.902	4.97	0.189	0.034	
Br $^- \cdots$ NH ₄ ⁺														
ϵ	Br \cdots H	Br \cdots N	H \cdots N	μ	ΔE	barrier	ϵ	Br \cdots H	Br \cdots N	H \cdots N	μ	ΔE	barrier	
1.0	1.937	3.037	1.100	10.73	1.81	4.12	5.0	2.236	3.278	1.042	14.11	-11.34	0.89	
2.0	2.063	3.128	1.065	12.30	-4.69	2.06	10.0	2.420	3.451	1.031	15.63	-15.32	0.34	
3.0	2.137	3.190	1.053	13.12	-8.13	1.12	15.0	+++	---	---	---	---	---	

^a Solute radius used in this calculation: 2.92 Å. ^b Radius used: 3.25 Å. ^c Radius used: 3.38 Å. ^d Radius used: 3.71 Å. ^e The “---” symbol indicates that only the neutral minimum is found and “+++” that the X⁻ and NH₄⁺ subsystems tend to infinitely separate.

$$\Delta E(X)^\ddagger = E(X^- \cdots H-NH_3^+)^\ddagger - E(X-H \cdots NH_3) \quad (4)$$

$$\Delta E(X) = E(X^- \cdots H-NH_3^+) - E(X-H \cdots NH_3) \quad (5)$$

This situation, with two wells of similar energy between

molecular complexes X-H \cdots NH₃ and ion-pair complexes X $^- \cdots$ H-NH₃⁺, can be explained by a low-barrier hydrogen bond based on the small energy barrier observed for most of the electric fields applied. These barriers decrease in all systems as the electric field increases.

TABLE 4: Hydrogen-Bonded Systems' Interatomic Distances (Å), Dipole Moments (μ , D), Electronic Density on the Bond Critical Points (ρ_c , e), and Relative Energies $\Delta E = E(X^{\dots}NH_4^+) - E(XH^{\dots}NH_3)$ (kcal mol⁻¹) of Molecular Complexes $XH^{\dots}NH_3$ and the Corresponding Zwitterions $X^{\dots}NH_4^+$ and Proton Transfer Barrier $\Delta E(X)^{\ddagger} = E(X^{\dots}H-NH_3^{\ddagger}) - E(X-H^{\dots}NH_3)$ Calculated with the 6-311++G Basis Set for Different External Electric Field Using Model B^b**

FH [⋯] NH ₃														
<i>q</i>	F [⋯] H	F [⋯] N	H [⋯] N	μ	$\rho_c(F^{\dots}H)$	$\rho_c(H^{\dots}N)$	<i>q</i>	F [⋯] H	F [⋯] N	H [⋯] N	μ	$\rho_c(F^{\dots}H)$	$\rho_c(H^{\dots}N)$	
0	0.918	2.738	1.820	4.60	0.358	0.036	400	0.964	2.584	1.620	6.20	0.295	0.062	
100	0.926	2.698	1.772	4.97	0.346	0.041	500	0.994	2.528	1.534	6.80	0.264	0.078	
200	0.935	2.664	1.730	5.35	0.332	0.046	560	+++						
300	0.947	2.627	1.680	5.75	0.316	0.052								
F ⁻ [⋯] NH ₄ ⁺														
<i>q</i>	F [⋯] H	F [⋯] N	H [⋯] N	μ	ΔE	barrier	<i>q</i>	F [⋯] H	F [⋯] N	H [⋯] N	μ	ΔE	barrier	
400	---						500	1.525	2.598	1.073	11.42	0.81	0.18	
ClH [⋯] NH ₃														
<i>q</i>	Cl [⋯] H	Cl [⋯] N	H [⋯] N	μ	$\rho_c(Cl^{\dots}H)$	$\rho_c(H^{\dots}N)$	<i>q</i>	Cl [⋯] H	Cl [⋯] N	H [⋯] N	μ	$\rho_c(Cl^{\dots}H)$	$\rho_c(H^{\dots}N)$	
0	1.291	3.306	2.015	4.19	0.243	0.026	200 ^a	1.978	3.035	1.056	12.72	0.044	0.290	
50	1.300	3.243	1.943	4.56	0.237	0.030	210 ^a	1.989	3.044	1.055	12.84	0.041	0.297	
100	1.308	3.219	1.911	4.89	0.232	0.033	250 ^a	2.064	3.110	1.046	13.51	0.034	0.306	
150	1.329	3.112	1.784	5.48	0.218	0.044	290 ^a	2.150	3.189	1.038	14.24	0.028	0.314	
180	1.345	3.071	1.726	5.86	0.209	0.051	330 ^a	2.304	3.334	1.031	15.35	0.019	0.323	
190 ^a	1.961	3.020	1.059	12.55	0.046	0.287								
Cl ⁻ [⋯] NH ₄ ⁺														
<i>q</i>	Cl [⋯] H	Cl [⋯] N	H [⋯] N	μ	ΔE	barrier	<i>q</i>	Cl [⋯] H	Cl [⋯] N	H [⋯] N	μ	ΔE	barrier	
50	1.765	2.880	1.114	10.42	3.21	4.06	150	1.909	2.978	1.069	12.00	-5.44	0.50	
100	1.832	2.920	1.088	11.20	-1.00	1.01	180	1.954	3.015	1.061	12.46	-8.15	0.02	
NCH [⋯] NH ₃														
<i>q</i>	C [⋯] H	C [⋯] N	H [⋯] N	μ	$r_c(C^{\dots}H)$	$\rho_c(H^{\dots}N)$	<i>q</i>	C [⋯] H	C [⋯] N	H [⋯] N	μ	$r_c(C^{\dots}H)$	$\rho_c(H^{\dots}N)$	
0	1.070	3.301	2.231	5.73	0.293	0.016	400	1.108	3.063	1.955	8.43	0.266	0.031	
100	1.075	3.264	2.189	6.35	0.289	0.018	500	1.134	2.978	1.844	9.33	0.248	0.040	
200	1.083	3.181	2.098	7.01	0.284	0.022	550	1.179	2.875	1.696	10.21	0.220	0.058	
300	1.094	3.127	2.034	7.69	0.278	0.024	560	+++						
NC ⁻ [⋯] NH ₄ ⁺														
<i>q</i>	C [⋯] H	C [⋯] N	H [⋯] N	μ	ΔE	barrier	<i>q</i>	C [⋯] H	C [⋯] N	H [⋯] N	μ	ΔE	barrier	
100	---						300	2.034	3.077	1.044	16.39	-2.13	2.21	
200	1.759	2.843	1.084	13.95	-12.84	13.64	400	+++						
BrH [⋯] NH ₃														
<i>q</i>	Br [⋯] H	Br [⋯] N	H [⋯] N	μ	$\rho_c(Br^{\dots}H)$	$\rho_c(H^{\dots}N)$	<i>q</i>	Br [⋯] H	Br [⋯] N	H [⋯] N	μ	$\rho_c(Br^{\dots}H)$	$\rho_c(H^{\dots}N)$	
0	1.428	3.518	2.090	3.96	0.200	0.023	160 ^a	2.141	3.192	1.052	13.19	0.038	0.296	
50	1.437	3.453	2.016	4.40	0.196	0.027	170 ^a	2.158	3.208	1.050	13.37	0.035	0.302	
100	1.451	3.368	1.917	4.94	0.190	0.033	190 ^a	2.158	3.208	1.050	13.37	0.035	0.302	
130	1.491	3.207	1.717	5.86	0.173	0.053	230 ^a	2.268	3.307	1.039	14.44	0.027	0.314	
140 ^a	2.111	3.167	1.056	12.87	0.039	0.296	270 ^a	2.385	3.417	1.032	15.41	0.021	0.321	
150 ^a	2.126	3.180	1.054	13.04	0.038	0.298								
Br ⁻ [⋯] NH ₄ ⁺														
<i>q</i>	Br [⋯] H	Br [⋯] N	H [⋯] N	μ	ΔE	barrier	<i>q</i>	Br [⋯] H	Br [⋯] N	H [⋯] N	μ	ΔE	barrier	
0	1.937	3.037	1.100	10.73	1.81	4.12	100	2.059	3.124	1.065	12.27	-7.92	0.50	
50	2.003	3.082	1.079	11.55	-2.92	2.01	130	2.097	3.155	1.058	12.72	-10.95	0.01	

^a The hydrogen has been transferred. ^b The “---” symbol indicates that only the neutral minimum is found and “+++” that the X⁻ and NH₄⁺ subsystems tend to infinitely separate.

As illustrated in Figure 2a, the calculated dipole moments increase in the initial stages in a linear way with the external electric field F . The larger increment corresponds to the more polarizable systems. Compared to $F = 0$, the dipole moment increase at $q = 100$ is 25% for BrH[⋯]NH₃, 17% for ClH[⋯]NH₃, 11% for NCH[⋯]NH₃, and 8% for FH[⋯]NH₃. At higher fields, again a monotonic nonlinear response is observed until, in the cases of Cl–H[⋯]NH₃ and Br–H[⋯]NH₃, sudden jumps are observed between $q = 100$ and 200. A look at Figure 2b indicates that these dipole moment jumps are associated with sudden changes of the proton-transfer coordinate $r_1 - r_2$. At

higher fields nonlinear monotonic increases of the dipole moments and the proton-transfer coordinates are observed again.

The similarity of the graphs in Figure 2 indicates that the dipole moment is a good measure of the proton location coordinate $r_1 - r_2$. The relation is almost linear as depicted in Figure 3a. Moreover, the slope of the curves obtained is similar for the molecular and the ionic complexes and almost independent of the chemical constitution.

Finally, we note some interesting geometric changes of the complexes depicted in Figure 3b where the heavy atom distances $r_1 + r_2$ are plotted as a function of the proton location coordinate

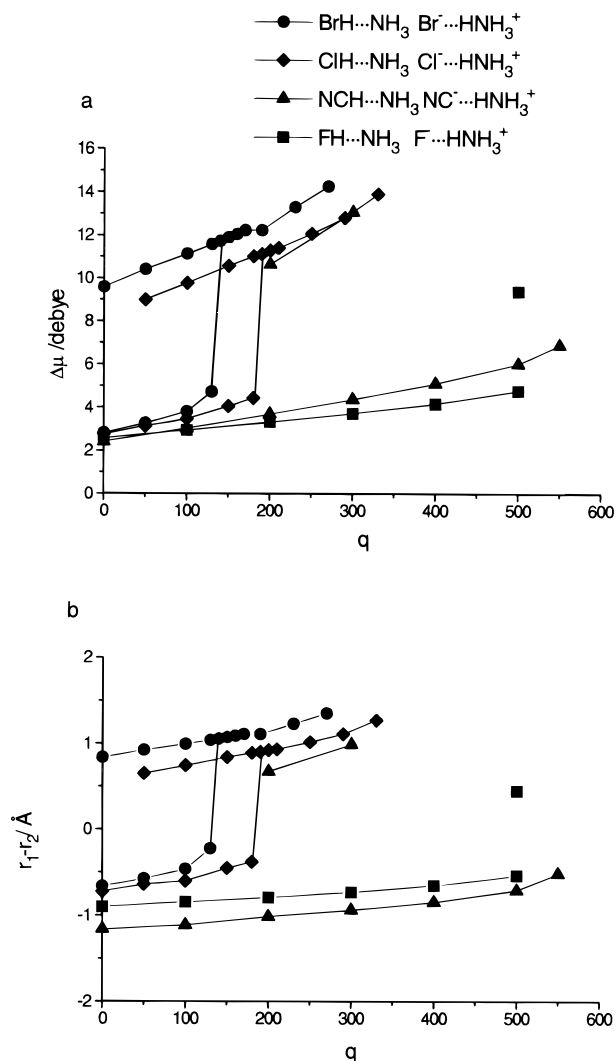


Figure 2. (a) Variation of the dipole moment $\Delta\mu = \mu_{\text{XHB}} - \mu_{\text{HX}}(0)$ of acid-ammonia complexes calculated in terms of model B using the 6-311++G** basis set as a function of the external electric field $F = 2qe_0/r_c^2 = 2.88 \times 10^5 q \text{ V cm}^{-1}$ in model B. $\mu_{\text{HX}}(0)$ represents the dipole moment of the free acid at $F = 0$. (b) Associated variation of the proton-transfer coordinate $r_1 - r_2$.

$r_1 - r_2$. When the electric field is increased, the hydrogen-bonded complexes strongly contract as $r_1 - r_2$ is increased i.e., as the proton is shifted toward the hydrogen bond center. In the ion-pair region, the increment of the field produces an expansion of the systems reflected by a simultaneous increment of the heavy atom distance $r_1 + r_2$ and the proton location coordinate $r_1 - r_2$.

The solid lines in Figure 3b were obtained using eq 3, by adapting the listed values of $(r_1 + r_2)_{\text{min}}$, setting the distance $\text{H}\cdots\text{N}$ in free ammonia to $r_{02} = 1.0118 \text{ \AA}$, and using the values r_{01} of the free donors in the absence of electric fields listed in Table 1. The fit is satisfactory ($r > 0.97$ in all the cases) in view of the crude model assumption of eq 1. We note that the minimum distance $(r_1 + r_2)_{\text{min}}$ is not realized in the ab initio calculations, since the proton is transferred at a larger transfer distance $(r_1 + r_2)_{\text{trans}}$.

In summary, the application of an external electric field F on XHB produces a correlated lengthening of the distance $\text{X}\cdots\text{H}$ and a shortening of the distance $\text{H}\cdots\text{B}$ in the molecular complexes and in the ion-pair complexes. This phenomenon is also reflected by the electron density of the critical bonds. The effect of the external electric field on the complexes prevents the calculation of the interaction energy (the difference

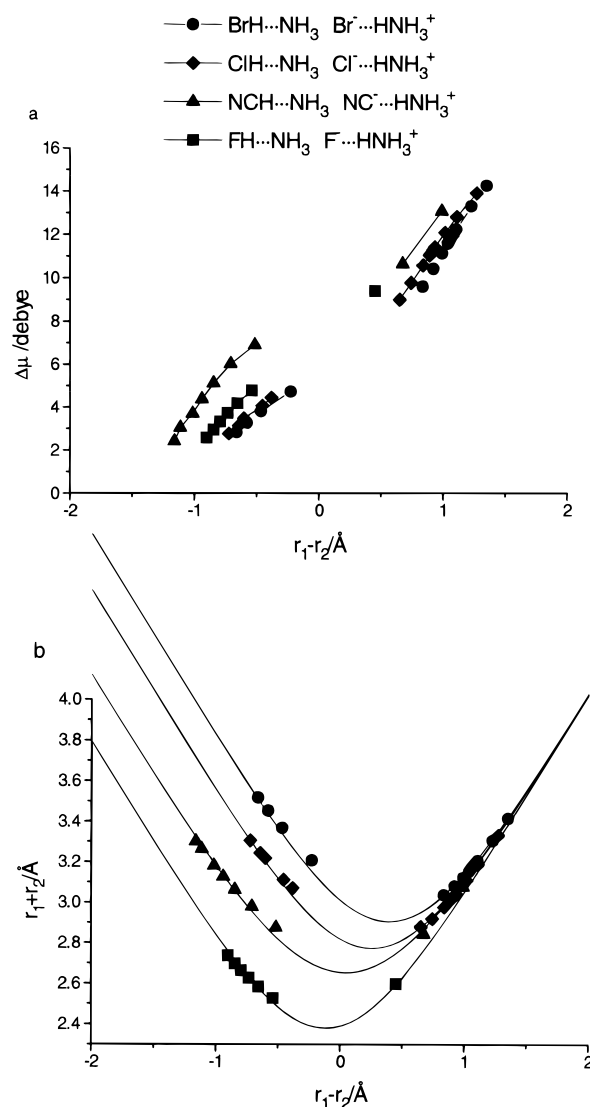


Figure 3. (a) Dipole moment $\Delta\mu$ variation as a function of the proton-transfer coordinate $r_1 - r_2$ calculated in terms of model B with the 6-311++G** basis set. (b) Field-induced correlation between the hydrogen bond heavy atom distance $r_1 + r_2$ and the proton-transfer coordinate $r_1 - r_2$. The solid lines were calculated using eq 3 using the values $r_{02} = 1.01 \text{ \AA}$, $r_{01} = 0.897, 1.058, 1.27, 1.407 \text{ \AA}$ and $(r_1 + r_2)_{\text{min}} = 2.39, 2.65, 2.81, 2.97 \text{ \AA}$ for $\text{HX} = \text{HF}, \text{HCN}, \text{HCl}, \text{HBr}$.

between the complex energy and the sum of the monomers energy) even when the energy of the monomers is evaluated in the presence of the electric field. However, on the basis of previous studies showing a linear relation between the electron density of the hydrogen bond critical points and the strength of this interaction,²⁵ the present results indicate that the hydrogen bond strength is greatly increased by a solvent dipole or a crystal field.

Results Obtained for Model A. As in model B, two minima are found; however, in this case any external electric field applied does not produce a conversion of the neutral systems to the corresponding ion pairs. The two local minima on the potential surface were found for $\text{X} = \text{Br}$ even at the smallest dielectric constant $\epsilon = 1.0$ corresponding to the molecular complex $\text{X}-\text{H}\cdots\text{NH}_3$ and the ion pairs form $\text{X}^-\cdots\text{H}-\text{NH}_3^+$, as indicated in Table 3. In the case $\text{X} = \text{F}$ and Cl , the zwitterionic form corresponds to a local minimum for $\epsilon = 2$, and the cyanide ionic complex appears at $\epsilon = 5.0$. For $\epsilon = 10$ the chloride and cyanide complexes tend to infinitely separate, which corresponds to the transformation of an intimate ion pair to a solvent-separated ion pair.²⁶ A similar observation of a

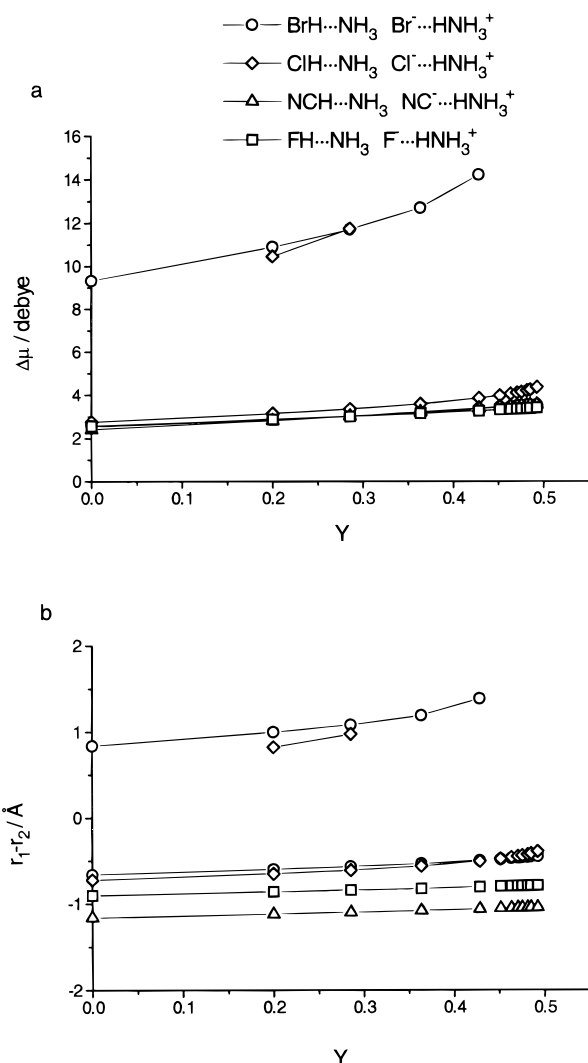


Figure 4. (a) Variation of the dipole moment $\Delta\mu = \mu_{\text{XHB}} - \mu_{\text{XH}}(0)$ of acid–ammonia complexes calculated in terms of model A using the 6-311++G** basis set as a function of the Onsager function $Y = (\epsilon - 1)/(2\epsilon + 1)$, where ϵ is the dielectric constant of the surrounding medium. (b) Associated variation of the proton-transfer coordinate $r_1 - r_2$.

zwitterionic form was made in ab initio calculations (MP2/6-31G**) of $X = \text{I}$ by Scheiner and Karr.⁸

The molecular and ion-pair complexes energetic barriers (eq 5) have been found to depend in a linear way on the Onsager function [$Y = (\epsilon - 1)/(2\epsilon + 1)$].^{27–29} By least-squares fitting, we obtained eqs 6 and 7:

$$\Delta E(\text{F}) = (47.8 \pm 0.6) - (52.1 \pm 2.2)Y, \quad n = 3, \\ r^2 = 0.998 \quad (6)$$

$$\Delta E(\text{Br}) = (2.4 \pm 0.8) - (39.0 \pm 2.7)Y, \quad n = 5, \\ r^2 = 0.986 \quad (7)$$

A direct comparison of these values with the values $\Delta E(\text{I})$ calculated by Scheiner and Karr⁸ is difficult, since the distances $X\cdots\text{N}$ were optimized here for each complex. By contrast, Scheiner et al. were interested in the energy profiles for the proton motion at several fixed distances $\text{I}\cdots\text{N}$. For short $\text{I}\cdots\text{N}$ distances, e.g., 3.21 Å, they found a single minimum corresponding to the ion pair [$\text{I}^-\cdots\text{H}\text{NH}_3^+$]. For longer $\text{I}\cdots\text{N}$ distances, e.g. 3.574 Å, two minima were observed, the most stable corresponding to the neutral complex and the less stable

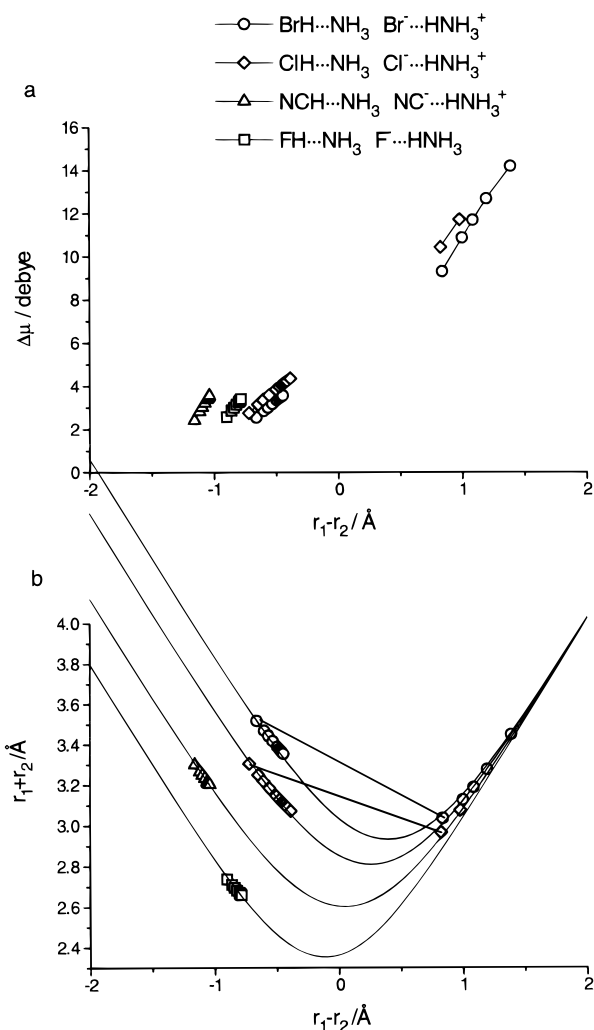


Figure 5. (a) Dipole moment $\Delta\mu$ variation as a function of the proton-transfer coordinate $r_1 - r_2$ calculated in terms of model A with the 6-311++G** basis set. (b) Field-induced correlation between the hydrogen bond heavy atom distance $r_1 + r_2$ and the proton-transfer coordinate $r_1 - r_2$. The solid lines are the same as in Figure 3b.

(by 2 kcal mol⁻¹) to the ion pair. They are separated by an energy barrier of about 5 kcal mol⁻¹.

Let us now compare the individual properties of the molecular and zwitterionic complexes summarized together in Figures 4 and 5. Each graph contains data points on the left-hand sides for the molecular complexes and on the right-hand sides for the coexisting zwitterions. As indicated in parts a and b of Figure 4, the dipole moments and the proton-transfer coordinates are much larger for the zwitterionic complexes compared to the molecular complexes. However, both quantities increase for both types of complexes as the Onsager function $Y = (\epsilon - 1)/(2\epsilon + 1)$ is increased. These increases are nonlinear and can be reproduced by second-order polynomials. These correlations show a new kind of relationship between molecular properties and the Onsager function, since previously only linear relationships were found.³⁰ Figure 5a shows again that dipole moments and the proton-transfer coordinates are related to each other although the relation is not as linear as in model B (Figure 3a).

The same field-induced geometric correlations between $r_1 + r_2$ and $r_1 - r_2$ of Figure 3b calculated for model B also hold in the case of model A, as depicted in Figure 5b. The inclusion of all the data in the same graph (Figure 6) shows that similar slopes and excellent correlation coefficients are found for each system studied.

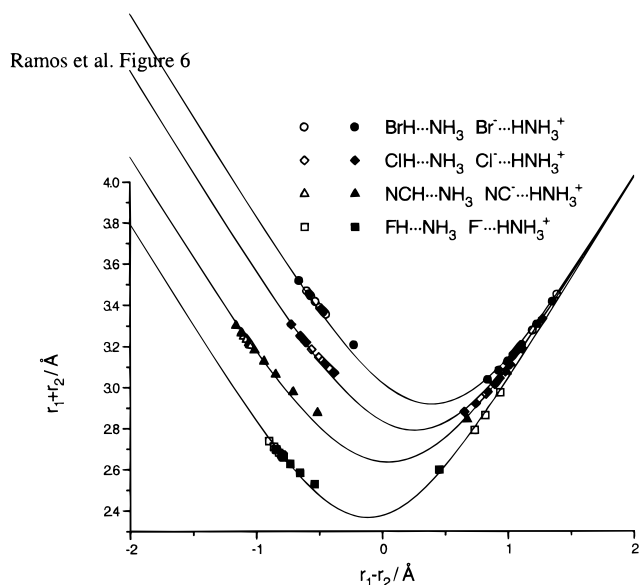


Figure 6. Field induced correlation between the hydrogen bond heavy atom distance $r_1 + r_2$ and the proton-transfer coordinate $r_1 - r_2$. Open dots indicates model A and the solid ones model B. The solid lines are the same as in Figure 3b.

Discussion

In the *ab initio* calculations presented above we have used two different ways in order to model the effects of a matrix electric field on the dipole moments and geometries of hydrogen-bonded 1:1 complexes of various acids $HX = HF, HCl, HBr,$ and HCN with ammonia. Particular attention was paid to the transformation of the molecular complexes $X-H\cdots NH_3$ to their corresponding zwitterionic forms $X^-\cdots H-NH_3^+$ which characterizes the acidity of the proton donor. In model A the solvent dielectric constant ϵ was increased using the Onsager reactive field formalism, whereas in model B a homogeneous electric field F was applied and continuously increased. This model was formulated on the grounds of the interpretation of intrinsic temperature-dependent NMR chemical shifts of various acid–base complexes at low temperatures.^{4c}

In both cases the electric interactions applied induce dipole moments in the molecular complexes by shifting the proton toward the base, i.e., by increasing the distance $X\cdots H \equiv r_1$ and decreasing the distance $H\cdots B \equiv r_2$. The difference $r_1 - r_2$ can conveniently be used as a proton-transfer coordinate, whereas the sum $r_1 + r_2$ characterizes the distance $X\cdots B$. When the electric field interactions in both models were varied and the proton shifted from X toward B, a correlation between $r_1 - r_2$ and $r_1 + r_2$ was found as indicated by the solid lines in Figures 3b and 5b, which were the same for both models. They indicate a hydrogen bond contraction to a minimum $X\cdots B$ distance $(r_1 + r_2)_{\min}$ that depends on the nature of X and B. Here, we obtained $(r_1 + r_2)_{\min} = 2.39, 2.65, 2.81, 2.97 \text{ \AA}$ for $HX = HF, HCN, HCl, HBr$. The minimum distance is reached at $(r_1 - r_2)_{\min} = r_{01} - r_{02}$ corresponding to the difference of the distances $X\cdots H$ and $H\cdots B$ in the free proton donors. Thus, in $O-H\cdots O$ and $N-H\cdots N$ hydrogen bonded systems $r_{01} \gg r_{02}$ and the shortest hydrogen-bond occurs for the symmetric bond with $r_1 - r_2 = 0$. Similar correlation curves $r_1 = f(r_2)$ have been established on the basis of neutron diffraction data of a variety of hydrogen-bonded solids by Steiner et al.^{3i,k} Here, these correlated hydrogen bond geometries are produced by varying the electric fields applied. At first sight it was surprising that these correlation curves are independent of the interaction model applied, as can be inferred from Figures 3b and 5b. However,

it is plausible that any interaction with the surrounding cannot lead to independent changes of the two distances.

In model B (Figure 3b) the increase of the electric field shifts the geometry on the correlation curve from the left- to the right-hand side in the neutral complex until the proton is transferred to the base. Thus, the gradual shift of the proton toward the hydrogen bond center is accompanied by the contraction of the system. As has been discussed recently,^{4c} this effect arises because of the polarizability of the lone pair of the base. When the electric field is increased, charge transfer from this lone pair to the acid occurs, creating a dipole moment, but the creation of a dipole moment by charge transfer is associated with a minimization of the distance between the charges created, i.e., here, with a contraction of the hydrogen bond. However, before the shortest $X\cdots B$ distance $(r_1 + r_2)_{\min}$ is reached, the proton is suddenly shifted across the hydrogen bond center. We associate this phenomenon to a kind of “corner cutting” arising from a double well potential for the proton motion around the transfer distance. In other words, $(r_1 + r_2)_{\min}$ refers to the most compressed geometry where the proton transfer is characterized by a single well potential; it could correspond to a stationary point with an imaginary frequency, i.e., to a transition state of proton transfer. When the electric field is further increased, the proton is shifted further toward B, and the hydrogen bond widens again. This is because now the dipole moment increase is mainly realized by increasing the distances between the existing positive and negative charges and not by creating new charges.

By contrast, as shown in Figure 5b, both the molecular complexes $X-H\cdots NH_3$ and their corresponding zwitterionic forms $X^-\cdots H-NH_3^+$ are present in model A and represent both stable states of different energy corresponding to local minima in the potential energy surface. As the dielectric constant is increased, both types of complexes experience similar geometric changes as in model B.

Thus, the acidity of a proton donor in terms of model A can be characterized as usual by an equilibrium constant K_a of proton transfer, i.e., a pK_a value, or by the dielectric constant ϵ which produces a constant of $K_a = 1$. On the other hand, in model B the acidity of the donor HX is characterized by the electric field F needed for compressing the hydrogen bond until the sudden proton transfer occurs starting from the neutral system, as indicated in Figure 3a. The electronic field needed to dissociate the HBr is smaller than for HCl , since HBr is a stronger acid. By contrast, HF is then a weak acid as a much larger field is required. This result agrees with the report of the X-ray diffraction of the first $FH\cdots N$ complex³⁰ in which the hydrogen is bonded to the halogen and not to the nitrogen.

The advantage of the acidity concept of model B is that it does not require any more proton transfer to be a kinetic process. In other words, model B is in principle more general and also applicable to acid–base complexes in enzymes, solids, and surfaces. We note, however, that model B is not complete, since in a normal polar solvent one must take into account a distribution of different electric fields leading to a distribution of hydrogen bond geometries. Moreover, depending on the experiments to which the model is to be applied, the particular time scale of the experimental method has to be taken into account; e.g., in NMR only one averaged environment can be observed and in kinetic experiments generally only a single rate constant of proton transfer. However, in IR or UV spectroscopy the exchange between different solvent sites is generally slow, and the spectra can be regarded as a static superposition of different solvent complexes exhibiting different local fields i.e., hydrogen bond geometries. Thus, in principle it should be

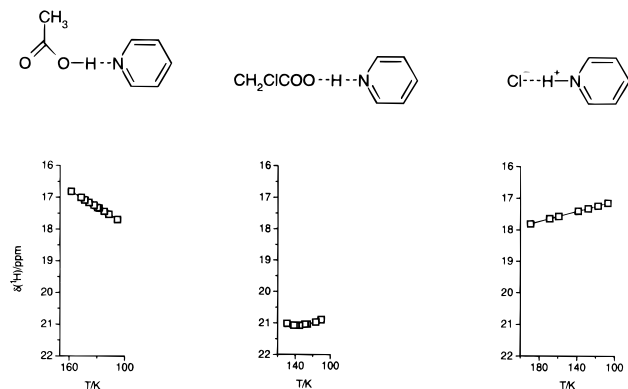


Figure 7. Intrinsic ^1H NMR chemical shifts of three 1:1 hydrogen bonded acid–pyridine complexes dissolved in a mixture of ($\text{CDF}_3/\text{CDF}_2\text{Cl}$ 2:1) reported recently.^{4c} These results indicate that the zwitterionic $\text{Cl}^- \cdots \text{pyridine}^+$ complex becomes shorter as temperature is increased and the molecular $\text{CH}_3\text{COOH} \cdots \text{pyridine}$ complex weaker. The shortest hydrogen bond is formed between Cl_3COOH and pyridine. The temperature effects are interpreted in terms of increasing electric field created by ordering of the solvent dipoles at low temperatures.

possible to obtain information on the distribution of the local fields, for example, of acid–pyridine complexes, by calculating the electronic transitions of pyridine as a function of the applied electric field and by UV or IR line shape analysis as a function of temperature.

On the other hand, one can conclude that the Onsager formalism used in model A should be equivalent to the assumption of a certain distribution of local electric fields in model B leading to different hydrogen bond geometries, where to each geometry a certain free energy is assigned.

Although the discussion of experimental support for one of the models is beyond the scope of this paper, let us only discuss some recent experimental findings^{4c} concerning acid–base complexes dissolved in polar solvents in terms of the findings of this study. In particular, low-temperature measurements of the intrinsic ^1H chemical shifts $\delta(^1\text{H})$ of three 1:1 acid–pyridine complexes in a mixture of two Freons ($\text{CDF}_3/\text{CDF}_2\text{Cl}$, 2:1) were reported^{4c} and are depicted in Figure 7. In previous studies of these systems the chemical shifts were averages over a variety of different hydrogen-bonded complexes. All acids, CH_3COOH , CCl_3COOH , and HCl form strong hydrogen bonds with pyridine as indicated by the low-field chemical shifts of the hydrogen-bonded protons. Under these conditions $\delta(^1\text{H})$ is a measure of the distance $r_1 + r_2$.^{4b} In the $\text{CH}_3\text{COOH} \cdots \text{pyridine}$ complex $d(^1\text{H})$ increases with decreasing temperature as $r_1 + r_2$ becomes smaller. The minimum distance $r_1 + r_2$, i.e., the highest value of $d(^1\text{H})$ is realized for the $\text{CCl}_3\text{COOH} \cdots \text{pyridine}$ complex at about 21 ppm. By contrast, $\delta(^1\text{H})$ of the $\text{Cl}^- \cdots \text{pyridine}^+$ complex is shifted to lower values as temperature is decreased, indicating a weakening of the hydrogen bond. The contrary, i.e., that a temperature increase weakens zwitterionic hydrogen bonds, had not been recognized before to our knowledge and could have some biological importance.

The similarity between the set of the three curves in Figure 7 with the correlation curves in Figure 3b is noticeable, and this similarity has been interpreted in terms of solvent dipole ordering at low temperatures, which increases the electric field at the hydrogen-bonded complexes studied.^{4c} The difference between the theoretical and experimental curves is that a sudden change as indicated in Figure 3 is not observed, but this can probably be ascribed to the distribution of electric fields in the experimental case. Thus, the results of this study clearly give further evidence for this interpretation. On the other hand, one could try to reproduce the experimental curves of Figure 7 by

calculating the NMR shielding surface as a function of the electric field applied and by taking the electric field distribution function from the UV spectra in the future.

Conclusions

The purpose of this study was to model using ab initio methods the effects of a polar environment on the dipole moments and geometry of low-barrier hydrogen-bonded acid–base complexes XHB. In previous studies (model A) the condensed media with a given dielectric constant have been modeled using the Onsager formalism. Here, we proposed an interesting alternative, i.e., to perform the calculations in the presence of a homogeneous (or of an inhomogeneous) electric field created by two distant opposite charges (Model B). The advantage of model Model B is that it can model low-barrier hydrogen-bonded systems in a solid environment, a surface, or in an individual solvent site on the time scale of slow solvent reorientation as indicated by the values of the proton-transfer barriers. Assuming a static distribution of electric fields at the solutes, experimental findings obtained recently by low-temperature NMR spectroscopy of acid–base complexes between organic acids and pyridine dissolved in polar solvents can be reproduced. Both models predict a field-induced correlation between the hydrogen bond distances $\text{X} \cdots \text{H}$ and $\text{H} \cdots \text{B}$ that can be used for an acidity concept based on hydrogen bond geometries rather than on proton-transfer equilibria.

Acknowledgment. This work has been supported by the EU network “Localization and Transfer of Hydrogen” (No. CHR X CT 940582), the Stiftung Volkswagenwerk, Hannover, and the Fonds der Chemischen Industrie, Frankfurt.

References and Notes

- (1) (a) Jeffrey, G. A.; Saenger, W. *Hydrogen Bonding in Biological Structures*; Springer-Verlag: Berlin, 1991. (b) Bell, R. P. *The Proton in Chemistry*, 2nd ed.; Chapman and Hall: London, 1973.
- (2) (a) Swain, C. G.; Kuhn, D. A.; Schowen, R. L. *J. Am. Chem. Soc.* **1965**, *87*, 1553. (b) Eliason, R.; Kreevoy, M. M. *J. Am. Chem. Soc.* **1978**, *100*, 7037. (c) Hadzi, D. Proton Transfers in Biological Mechanisms. *J. Mol. Struct.* **1988**, *177*, 1. (d) Cleland, W. W.; Kreevoy, M. M. *Science* **1994**, *264*, 1887. (e) Perrin, C. L. *Science* **1994**, *266*, 1665. (f) Blow, D. M.; Birktoft, J. J.; Hartley, B. S. *Nature* **1969**, *221*, 337. (g) Blow, D. M.; Steitz, T. A. *Annu. Rev. Biochem.* **1970**, *39*, 63. (h) Schowen, R. L. In *Mechanistic Principles of Enzyme Activity*; Liebman, J. F., Greenberg, A., Eds.; VCH Publishers: New York, 1988; p 119. (i) Schowen, K. B.; Schowen, R. L. *Methods Enzymol.* **1982**, *87*, 551. (j) Venkatasubban, K. S.; Schowen, R. L. *CRC Crit. Rev. Biochem.* **1984**, *17*, 1. (k) Cook, P. F. *Enzyme Mechanisms from Isotope Effects*; CRC Press: New York, 1992.
- (3) (a) Frey, P. A.; Whitt, S. A.; Tobin, J. B. *Science* **1994**, *264*, 1927. (m) Denisov, G. S.; Golubev, N. S.; Gindin, V. A.; Limbach, H. H.; Ligay, S. S.; Smirnov, S. N. *J. Mol. Struct.* **1994**, *322*, 83. (n) Golubev, N. S.; Gindin, V. A.; Ligay, S. S.; Smirnov, S. N. *Biochemistry (Moscow)* **1994**, *59*, 447.
- (4) (a) Schuster, P.; Zundel, G.; Sandorfy, C. Eds., *The Hydrogen Bond*; North-Holland Publ. Co.: Amsterdam, 1976. (b) Kreevoy, M. M.; Liang, T. M. *J. Am. Chem. Soc.* **1980**, *102*, 361. (c) Emsley, J.; Jones, D. J.; Lucas, J. *Rev. Inorg. Chem.* **1981**, *3*, 105. (d) Ault, B. S. *Acc. Chem. Res.* **1982**, *15*, 103. (e) Mootz, D.; Bartmann, K. *Angew. Chem.* **1988**, *100*, 424; *Angew. Chem. Int. Ed. Engl.* **1988**, *27*, 391. (f) Berthold, H. J., Preibsch, E.; Vonholdt, E. *Angew. Chem.* **1988**, *100*, 1581; *Angew. Chem. Int. Ed. Engl.* **1988**, *27*, 1527. (g) Hibbert, F.; Emsley, J. *Adv. Phys. Org. Chem.* **1980**, *26*, 255. (h) Novak, A., *Struct. Bonding (Berlin)* **1974**, *18*, 177. (i) Steiner, Th.; Saenger, W. *Acta Crystallogr.* **1994**, *B50*, 348. (k) Steiner, Th. *J. Chem. Soc. Chem. Commun.* **1995**, 1331. (l) Gilli, P.; Bertolasi, V.; Ferretti, V.; Gilli, G. *J. Am. Chem. Soc.* **1994**, *116*, 909.
- (4) (a) Golubev, N. S.; Smirnov, S. N.; Gindin, V. A.; Denisov, G. S.; Benedict, H.; Limbach, H.-H. *J. Am. Chem. Soc.* **1994**, *116*, 12055. (b) Smirnov, S. N.; Golubev, N. S.; Denisov, G. S.; Benedict, H.; Schah-Mohammedi, P.; Limbach, H.-H. *J. Am. Chem. Soc.* **1996**, *118*, 4094. (c) Golubev, N. S.; Denisov, G. S.; Smirnov, S. N.; Shchepkin, D. N.; Limbach, H.-H. *Z. Phys. Chem.* **1996**, *196*, 73.

- (5) Scheiner, S.; Redfern, P.; Szczesniak, M. M. *J. Phys. Chem.* **1985**, *89*, 262.
- (6) Eckert, M.; Zundel, G. *J. Phys. Chem.* **1987**, *91*, 5170.
- (7) Scheiner, S.; Kurnig, I. *J. Int. J. Quantum Chem., Quantum Biol. Symp.* **1987**, *14*, 47.
- (8) Scheiner, S.; Kar, T. *J. Am. Chem. Soc.* **1995**, *117*, 6970.
- (9) Corongiu, G.; Estrin, D.; Murgia, G.; Paglieri, L.; Pisani, L.; Suzzi Valli, G.; Watts, J. D.; Clementi, E. *Int. J. Quantum Chem.* **1996**, *59*, 119.
- (10) Onsager, L. *J. Am. Chem. Soc.* **1936**, *58*, 1486.
- (11) Benedict, H.; Hoelger, C.; Aguilar-Parrilla, F.; Fehlhammer, W. P.; Wehlan, M.; Janoschek, R.; Limbach, H.-H. *J. Mol. Struct.* **1996**, *378*, 11.
- (12) Hariharan, P. C.; Pople, J. A. *Theor. Chim. Acta.* **1973**, *28*, 213.
- (13) Krishnam, R.; Binkley, J. S.; Seeger, R.; Pople, J. A. *J. Chem. Phys.* **1984**, *80*, 3265.
- (14) Wong, M. W.; Wiberg, K. B.; Frisch, M. J. *J. Comput. Chem.* **1995**, *16*, 385.
- (15) Frisch, M. J.; Trucks, G. W.; Schlegel, H. B.; Gill, P. M. W.; Johnson, B. G.; Robb, M. A.; Cheeseman, J. R.; Keith, T.; Petersson, G. A.; Montgomery, J. A.; Raghavachari, K.; Al-Laham, M. A.; Zakrzewski, V. G.; Ortiz, J. V.; Foresman, J. B.; Cioslowski, J.; Stefanov, B. B.; Nanayakkara, A.; Challacombe, M.; Peng, C. Y.; Ayala, P. Y.; Chen, W.; Wong, M. W.; Andres, J. L.; Replogle, E. S.; Gomperts, R.; Martin, R. L.; Fox, D. J.; Binkley, J. S.; Defrees, D. J.; Baker, J.; Stewart, J. P.; Head-Gordon, M.; Gonzalez, C.; Pople, J. A. *Gaussian-94*; Gaussian, Inc.: Pittsburgh, 1995.
- (16) Hirschfelder, J. O.; Curtiss, C. F.; Bird, R. B. *Molecular Theory of Gases and Liquids*, 4th ed.; John Wiley & Sons: New York, 1967.
- (17) Dupuis, M.; Maluendes, S. A. In *MOTECC: Modern Techniques in Computational Chemistry*; Clementi, E., Ed.; ESCOM Science: Leiden, 1991.
- (18) Bader, R. F. W. *Atoms in Molecules: A Quantum Theory*; Oxford University Press: Oxford, 1990.
- (19) Ciolowski, J.; Nanayakkara, A. *Chem. Phys. Lett.* **1994**, *219*, 151 and references therein.
- (20) Brown, I. D. *Acta Crystallogr.* **1992**, *B48*, 553.
- (21) Wong, M. W.; Frisch, M. J.; Wiberg, K. B. *J. Am. Chem. Soc.* **1991**, *113*, 4776.
- (22) Wong, M. W.; Wiberg, K. B.; Frisch, M. J. *J. Am. Chem. Soc.* **1992**, *114*, 1645.
- (23) Wiberg, K. B.; Wong, M. W. *J. Am. Chem. Soc.* **1993**, *115*, 1078.
- (24) Paglieri, L.; Corongiu, G.; Estrin, D. A. *Int. J. Quantum Chem.* **1995**, *56*, 615.
- (25) Wiberg, K. B.; Rablen, P. R.; Rush, D. J.; T. A. Keith, *J. Am. Chem. Soc.* **1995**, *117*, 4261.
- (26) March, J. *Advanced Organic Chemistry*, 4th ed.; John Wiley & Sons: New York, 1992; p 302.
- (27) Koppel, I. A.; Palm, V. In *Advances in Linear Free Energy Relationships*; Chapman, N. B., Shorter, J., Eds.; Plenum Press: Oxford, 1992; p 116.
- (28) Paéz, J. A.; Campillo, N.; Elguero, J. *Gazz. Chim. Ital.* **1996**, *126*, 307.
- (29) A model of the form $\Delta E = a_0 + a_1Y + a_{11}Y^2$ yields r^2 values = 1.000.
- (30) Jiao, H.; von R. Schleyer, P. *J. Am. Chem. Soc.* **1994**, *116*, 7429.